Materials International
Open-Access Journal (ISSN: 2668-5728)

Review
Volume 7, Issue 4, 2025, 36
https://doi.org/10.33263/Materials74.036

Genotoxicity and Reactive Oxygen Species-Inducing Potential of Silver Nanoparticles Synthesized using *Calotropis gigantea* Extracts in Laboratory Mice

Mohammed Ahmed Hussein Awad [1,*], Yasmin M.S. Jamil [2], Ahmed Ali Al-kawmani [3], Hussein M.A. Al-Maydama [2]

[1] Chemistry Department, Faculty of Applied Sciences, Thamar University, Thamar, Yemen
[2] Department of Chemistry, Faculty of Science, Sana'a University, Yemen
[3] Agriculture Department, Faculty of Agriculture and Veterinary Medicine, Thamar University, Thamar, Yemen
* Correspondence: mohammed.awad@tu.edu.ye;

Received: 22.03.2025; Accepted: 23.07.2025; Published: 12.10.2025

Abstract: Medicinal plants that contain antioxidants such as flavonoids and phenolic compounds have gained much attention in the medical field. *Calotropis gigantea* is one of the most important plants rich in these compounds. In this study, silver nanoparticles were prepared with antioxidants obtained from *C. gigantea* (CgAgNPs) leaf extract and investigated for their improvement potential against reactive oxygen species (ROS), cytotoxicity, and genotoxicity, including the antioxidant activity of CgAgNPs. The study was conducted on 18 groups of SWR/J mice, each group consisting of six mice selected randomly. The control group was administered 1 mg/kg body weight (bw) of distilled water and positive control group was given only one dose of silver nanoparticles (AgNPs) below LD50 value of 50 mg/kg bw, followed by three doses of CgAgNPs (100, 150, and 200 mg/kg bw) at 24 h, 48 h, and 72 h, respectively. The results showed a significant increase in ROS levels in the positive control group, owing to AgNPs' ability to induce oxidative stress; chromosomal aberrations and increased micronuclei incidence were also observed. Also, the effects of CgAgNPs were confirmed by reduced genotoxicity, lower oxidative stress levels, and decreased ROS, chromosome aberrations, and micronuclei. In conclusion, these results demonstrate that CgAgNPs exert significant protective effects against AgNPs-induced toxicity in experimental mice through their antioxidant activity.

Keywords: antioxidant; silver nanoparticles; synthesis; reactive oxygen species; genotoxicity; *Calotropis gigantea*.

1. Introduction

Recently, advancements in nanotechnology have attracted significant attention to nanomaterials (NMs) owing to their higher surface area-to-volume ratios compared to bulk materials, with sizes in the nanometer range (1–100 nm), resulting in significant increases in catalytic and biological activity [1]. Nanostructures, including zero-dimensional (0D), one-dimensional (1D), two-dimensional (2D), and three-dimensional (3D) configurations, have attracted particular attention owing to their unique properties and potential for innovative applications [2–5].

The synthesis of silver nanoparticles (AgNPs) using plant extracts has drawn increasing interest among researchers due to their eco-friendly, non-pathogenic, and cost-effective nature. Silver ions interact with plant-derived compounds such as amino acids, proteins, enzymes, alkaloids, polysaccharides, phenolics, tannins, terpenoids, vitamins, and saponins, which not only facilitate reduction and stabilization but also impart medicinal properties [6–8].

Calotropis gigantea is a species from the genus Calotropis, a shrub that grows up to 4 m tall and bears white or lavender flowers. Due to the potent biological activity of calotropin, *C. gigantea* is a widely used medicinal plant in traditional systems of medicine across countries like Saudi Arabia and Yemen [9]. It is known for its protective effects against reactive oxygen species (ROS) and is used to treat a variety of conditions, including skin, digestive, respiratory, circulatory, and neurological disorders, as well as elephantiasis, fever, nausea, vomiting, and diarrhea [10,11]. Additionally, chloroform extracts from its leaves exhibit considerable antidiabetic activity [12].

While the traditional uses of *C. gigantea* are well documented, there is a clear need for *in vivo* studies to evaluate its safety and therapeutic potential [13]. Several studies have reported its cytotoxic activity against colon (HCT-116), lung (A549), and liver (HepG2) cancer cell lines [14,15], emphasizing the importance of further pharmacological exploration. The leaves, roots, and flowers of *C. gigantea* have also been utilized to synthesize AgNPs, which have shown promising results in anticancer, antibacterial, antioxidant, antifungal, antiviral, and antidiabetic applications [16–18].

Although the green synthesis of AgNPs using *C. gigantea* has been established [19–21], limited data are available comparing their safety profile with that of chemically synthesized AgNPs. Chemically synthesized AgNPs have been associated with adverse biological effects, including cytotoxicity, oxidative stress, and genotoxicity, which are influenced by their size, shape, concentration, and surface chemistry [22–24]. Recent studies have demonstrated that green-synthesized AgNPs, particularly those mediated by plant extracts, tend to exhibit reduced toxicity due to natural capping agents that modulate their interactions with biological systems [25–27]. However, these comparative findings remain scarce, especially *in vivo*.

The toxic effects of AgNPs in rats have included cytotoxic and genotoxic impacts on kidney and liver cells, increased chromosome breaks, and polyploidy [22]. These effects can persist due to the long biological half-life of AgNPs [24]. Other in vitro studies report AgNP toxicity in neutrophils [25–27], macrophages [28], Sertoli and granulosa cells [29], and even in Drosophila [30].

In aquatic models, green-synthesized AgNPs induced fewer alterations in hematological and hepatic biomarker profiles in Hypophthalmichthys molitrix than chemically synthesized AgNPs [31]. Similar assessments in juvenile clams (Mercenaria mercenaria) revealed lower toxicity of biologically synthesized AgNPs than chemically prepared ones, when normalized to equivalent total silver concentrations [32].

Thus, to achieve safe use of AgNPs as a medical treatment in humans, the present study was designed to explore the synthesis of CgAgNPs using *C. gigantea* plant extracts and to explore their potential improvement action against oxidative stress, cytotoxicity, and genotoxicity induced by AgNPs. Moreover, the safety and toxicity of *C. gigantea* extracts were studied in an experimental animal model (laboratory mice), thereby contributing to the growing field of green nanotechnology and its biomedical applications.

2. Materials and Methods

2.1. Collection of plant materials and extraction.

Leaves of *C. gigantea* were collected from its natural habitat in some regions of Yemen, and the plant was identified by consulting the documentation on the flora of Yemen. The herbarium specimens obtained were housed at TUH (Thamar University, Agriculture Department, Faculty of Agriculture and Veterinary, Thamar, Yemen). The collected leaves were rinsed thoroughly with tap water, cut into small pieces, oven-dried at 50°C, and finally ground into a powder. The methanol leaves extract of *C. gigantea*, and powder were prepared [33-35], and combined with silver nanoparticles (AgNPs) as described in a previous study [36].

2.2. The chemical composition.

The chemical composition of the methanol leaves extract using GC-MS/MS analysis. According to the method reported by Stankov-Jovanović *et al*. [37]. Briefly, the analysis was carried out using a GC (Agilent Technologies 7890A) interfaced with a mass-selective detector (MSD, Agilent 7000 Triple Quad) equipped with Agilent HP-5ms (5%-phenyl methyl poly siloxane) capillary column (30 m × 0.25 mm i.d. and 0.25 μm film thickness).

2.3. Total phenolics and Total flavonoids.

Also, the total phenolic and total flavonoid contents of the methanol leaf extract of C. gigantea were determined using methods [33, 34]. The absorbance was determined at 765 nm and 415 nm, respectively. Total phenolic compounds were expressed as equivalents of gallic acid per gram of dry extract weight (mgGAE/gextract). Total flavonoid contents were expressed as quercetin equivalent/g of sample (mgQE/g) [33, 38].

2.4. Antioxidant activity.

The methanol DPPH radical scavenging activity was described using a method [33]. Standard ascorbic acid solution (1mg/ml) and test sample solutions (1mg/ml) of methanol leaves extract of *C. gigantea* [33]. 1ml of 0.3mM DPPH solution was added to 2ml of each at concentrations of 10, 15, 25, 50, 75, and 100 of ascorbic acid, methanol leaves extract of *C. gigantea*, and CgAgNPs. Then, the incubated at dark for 30 minutes at room temperature after it was vigorously shaken. Absorbance was measured at 517 nm, with methanol as the blank, using UV-Visible spectroscopy. The percentage of inhibition and the IC_{50} value were calculated by [33, 11].

2.5. AgNPs.

Silver nanoparticles of size ≤ 100 nm and approximately 99.5% trace metals basis were purchased from Sigma-Aldrich (St. Louis, MO, USA).

2.6. Characterization.

Changes in color were recorded by periodic sampling and scanning using UV-visible spectrophotometry (BioTek, Winooski, VT, USA) over wavelengths ranging from 300 to 700 nm for up to 150 minutes. Transmission electron microscopy (TEM) was performed using a JEM 1101 transmission electron microscope (JEOL, Tokyo, Japan) to confirm the shape and

size of the AgNPs. The samples were dispersed in ethanol on a carbon-coated copper (TEM) grid. The images were obtained at an accelerating voltage of 120 kV. The crystalline structures of the synthesized CgAgNPs were investigated by X-ray diffraction (XRD). Lyophilized and powdered samples were used, and the diffraction patterns were recorded in the scanning mode using an X'pert Pro X-ray diffractometer (PANalytical, Almelo, The Netherlands) operating at 40 kV, 30 mA, and Cu-Kα radiation (α = 1.5418 Å) in the range of 20–80° in 2θ angles. XRD was also used to verify the crystal structure of the synthesized AgNPs.

2.7. Animals, treatments, and experimental design.

In vivo experiments were conducted using inbred SWR/J mice of either sex, ranging from 10 to 12 weeks old and weighing approximately 28–30 mg. Mice were obtained from the experimental mice facility of the Department of Agriculture, Faculty of Agriculture and Veterinary, Thamar University. The experiments were conducted per the guidelines of the Animal Ethics Committee at Thamar University (Ethics References No. SE-19-127). Mice were acclimatized for 1 week before starting the experiments in an environmentally controlled room maintained at a temperature of 23 ± 2°C, relative humidity of 44 ± 6%, and a dark/light cycle of 11/15 h. Rodent chow (commercially available in Yemen) and water were offered ad libitum.

A short-term acute toxicity test was conducted in mice to determine the LD50 dose of AgNPs, CgAgNPs, and *C. gigantea* extract. The LD_{50} value (100, 240, and 350 mg/kg BW) was found, respectively. The experiment was carried out on 18 groups of SWR/J mice, each group consisting of six mice selected randomly. The control group was given 1 mg/kg body weight (bw) of distilled water via gavage for 24, 48, and 72 h. One dose of AgNPs (50 mg/kg bw) below the LD_{50} value was administered to the positive control groups at 24, 48, and 72 h to establish their oxidative stress, genotoxicity, and cytotoxicity in mice. Subsequently, mice were treated with three safe doses of CgAgNPs (100, 150, and 200 mg/kg bw) for 24, 48, and 72 h, respectively. Finally, one dose of *C. gigantea* extract (300 mg/kg bw) below the LD_{50} value was administered in the negative control groups for three different durations (24, 48, and 72 h).

2.8. ROS.

After completing the trial period, the mice were sacrificed by administering a lethal dose of chloroform. The mice were then dissected, and 100 mg of liver was weighed and thoroughly washed in 1 mL 70% saline solution three times. The liver sample was cut into fine pieces and then ground in a ceramic container. The crushed sample was washed with 500 µl of 1×PBS and centrifuged at 7500×g for 10 min to aid cell retention. This step was repeated 2-3 times. In the last wash, the clarifier was discarded, and 100 µL of fresh 1×PBS was added with 10 µL of H2DCFDA dye (Image-iT™ LIVE Green Reactive Oxygen Species Detection Kit, Molecular Probes, USA), followed by incubation in a water bath for 35 min. Next, we centrifuged the sample at 7500×g for 10 min, discarded the dye, and added 400 µL of fresh 1× PBS. Finally, 20 µL of the stained cells were examined under a fluorescence microscope (Olympus® BX41, Olympus, Tokyo, Japan) at a magnification of 400×. For quantitative analysis, 400 µL of the cell suspension was transferred to a 96-well plate (100 µL/well).

ROS intensity was measured with a microplate reader at 485 nm excitation and 528 nm emission. Fluorescence readings were averaged across multiple wells and presented as a percentage relative to the control group.

2.9. Chromosome aberrations.

After completing the time periods for each dose per the experiment design, the mice were injected with 0.5 mL of 0.05% colchicine. The mice were sacrificed 90 min later, with an overdose of chloroform. Their bone marrow cells were collected from the femur bones by flushing with 0.075% normal saline. Subsequent slide preparation and analysis of the chromosomes followed the procedures described by [30]. The mitotic index (MI) for each treatment was determined, and numerical aberrations were analyzed under an Olympus® BX41 microscope using the 100× oil immersion objective lens [39].

2.10. Micronucleus (MN) test.

Subsequent slide preparation and analysis of the chromosomes followed the procedures described by [39]. All experiments were performed in triplicate to ensure the reproducibility of data. The data were presented as mean ± standard error (SE). Depending on the experiment, a two-tailed Student's least significant difference or two-way analysis of variance was applied to determine the significance of the data (depending on the experiment), and results with P values < 0.05 were considered statistically significant. Statistical analyses were performed using SPSS Statistics software (SPSS Inc., Chicago, IL, USA).

2.11. TUNEL assay (apoptosis).

Liver tissue sections obtained from treated and control mice were used for DNA fragmentation detection by using a TUNEL assay kit (TUNEL Universal apoptosis detection kit-FITC labeled, Gene Script, USA). Subsequent slide preparation and analysis of the apoptosis followed the procedures described by [39].

2.12. Statistical analysis.

All experiments were performed in triplicate to ensure the reproducibility of data. The data were presented as mean ± standard error (SE). A two-tailed Student's LSD or two-way ANOVA was applied to determine the significance of the data (depending on the experiment), and results with P values < 0.05 were considered statistically significant. Analyses of statistics were performed by the SPSS statistical analysis system (SPSS Inc., Chicago, IL, USA).

3. Results and Discussion

3.1. Extract and the chemical composition.

The different phytol-components present in the methanol leaves extract of the *C. gigantea* were identified using GC-MS as summarized in Figure 1A. The leaves extract of the *C. gigantea* contained trans-tetrahydrofuran-3,4-diol (0.22); glycerin (0.35); α-L-galactopyranoside, methyl-6-deoxy (11.28); 2-p-nitrobenzoyl1,3,5-tribenzyl-α-D-ribose (1.57); 1,3-butadiene-1-carboxylic acid (4.04); 7-Hydroxyfarnesen (4.42); 5,7,3',4',5'-Pentamethoxyflavone (3.42); 6,4'-Dimethoxy-7-hydroxyisoflavone (2.11); ethanedioic acid, bis(trimethylsilyl) (7.01); cyclopentane undecanoic acid, methyl (3.15); 3-nitropropanoic

acid(2.23); butoxyacetic acid (31.11); 4',6-Dimethoxyisoflavone-7-O-β-D-glucopyranoside (3.23); 7-nonenoic acid, methyl (5.63); 3-decen1-ol, (E) (19.11); 3,5-dimethyl-5-hexen-3-ol(1.12) [33, 34].

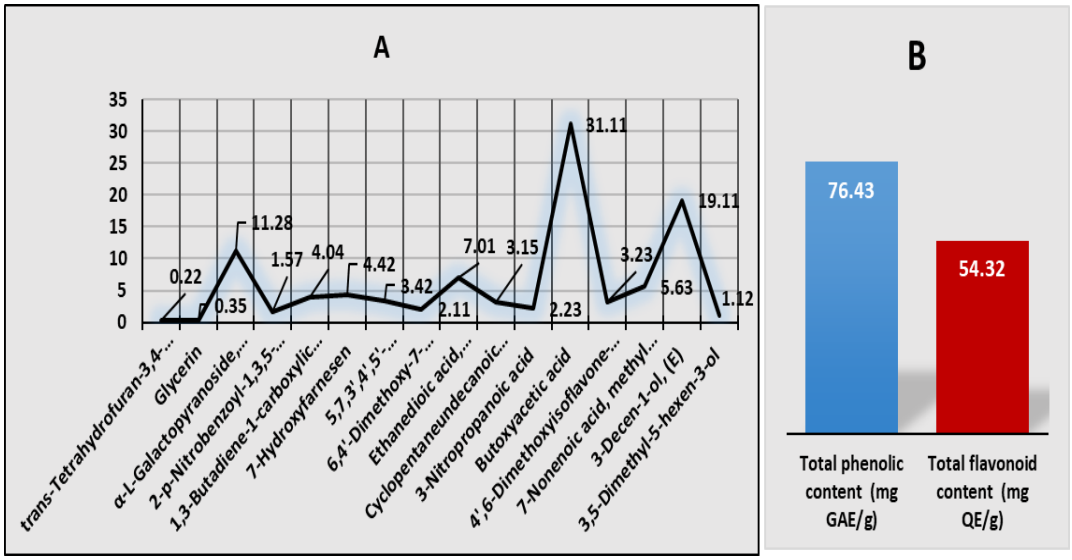

Figure 1. (A) Total compound contents of the methanolic leaves extract of *C. gigantea* by GC-MS analysis; **(B)** Total phenolic and flavonoid contents of the methanol extract of *C. gigantea.* The absorbance was determined at 765 nm and 415 nm, respectively.

3.2. Total phenolics and total flavonoids.

The total phenolic and flavonoid contents of *C. gigantea* leaf extracts are summarized in Figure 1 B. The results indicate that the methanolic extract of *C. gigantea* leaves exhibited a higher total phenolic content of 76.43 ± 2.54 mg GAE/g of extract, while the total flavonoid content was 54.32 ± 2.41 mg QE/g, which was comparatively lower than the phenolic content. Phenolic and flavonoid compounds in methanolic extracts of *C. gigantea* leaves are important dietary components known to possess antioxidant activity in biological systems by scavenging reactive free radicals [37]. Flavonoids represent the largest class of phenolic compounds, constituting more than half of all naturally occurring phenolics [34, 37]. Biochemical screening tests confirmed the presence of glycoside-linked tannins and flavonoids in the plant extracts, further supporting that the observed bioactivities in this study are largely attributed to phenolic and flavonoid compounds [33, 34, 37].

3.3. Antioxidant activity.

The antioxidant activity of methanol leaves extract (*C. gigantea)* and CgAgNPs was evaluated by using commonly employed DPPH radical scavenging assays (2,2-diphenyl-1-picrylhydrazyl). Radical scavenging effect of the plant on DPPH radicals was expressed as % inhibition (percentage inhibition) and compared with that of ascorbic acid, as shown in Figure 2. As per the IC_{50} values, the antioxidant activity of the methanol leaves extract (*C. gigantea*), CgAgNPs, and ascorbic acid was observed (48.97±1.46, 17.98±1.23, and 31.21±1.03 µg/ml), respectively. The plant extract contains various primary and secondary metabolites like carbohydrates, phenolic compounds, tannins, flavonoids, saponins, terpenoids, and steroids. Therefore, these bioactive ingredients have the capability to discolor the DPPH solution [33, 34]. In the hydrogen peroxide assay, hydroxyl radicals are generated and may lead to cytotoxicity [33]. Thus, any component can scavenge hydrogen peroxide and may protect the living being [34, 35]. Such activities are reliant on the concentration of the extracts. It is

concluded that the antioxidant property of the plant may be due to the polyphenolic components [35].

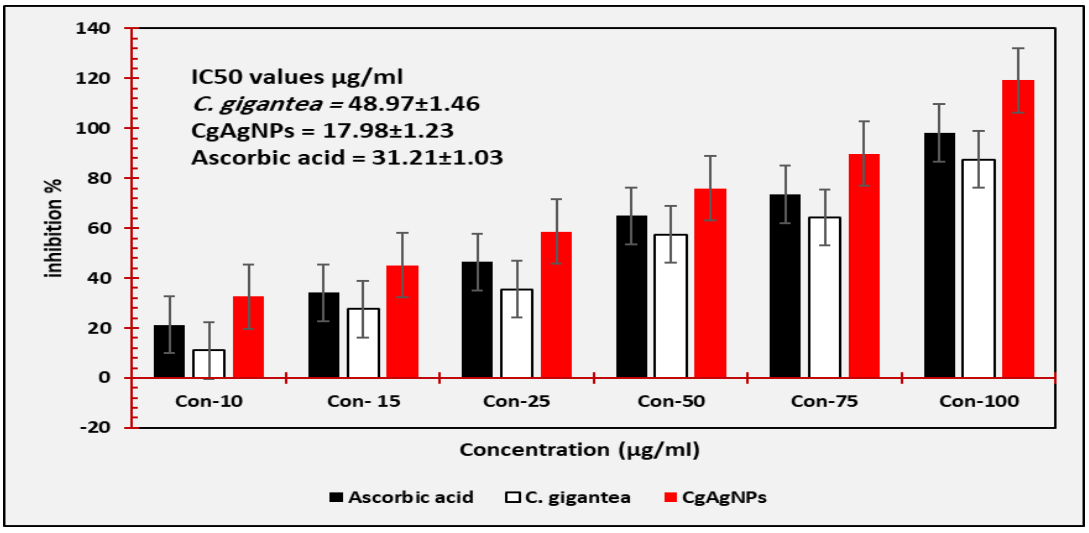

Figure 2. DPPH free radical scavenging assay of *C. gigantea*, CgAgNPs, and ascorbic acid. % inhibition: percentage inhibition. As per the IC_{50} values, the antioxidant activity of *C. gigantea*, CgAgNPs, and ascorbic acid.

3.4. Synthesis and characterization.

C.gigantea plant leaves were successfully used in the synthesis of AgNPs. Upon completion of mixing the aqueous methanol leaves extract and silver nitrate solution ($AgNO_3$), the color changed from pale yellow to brown (Figure 3A) for 150 minutes, which indicates that *C. gigantea* extract accelerates CgAgNPs synthesis. These effects were examined using UV-visible spectroscopy of CgAgNPs, which showed an absorption peak at 406.00 nm (Figure 3B). Strong resonance centered at 406–450 nm wavelength was clearly observed with increasing intensity over time; this may arise because of the interaction of silver ions with the components of *C. gigantea* plant, such as cardiac glycosides, amides [18], antioxidants such as phenolics, flavonoids, lipid peroxides, calcium oxalate, and fatty acids [33]. During CgAgNPs synthesis, the color change from yellowish to brown (approximately 150 minutes) proved that *C. gigantea* extract accelerates the CgAgNPs synthesis process. The acceleration of the synthesis process may be due to strong surface vibrations of a longitudinal plasmon in the AgNPs solution during the reaction process. This explanation aligns with many previous studies that suggest that a surface-vibration process of a plasmon accelerates the synthesis of silver nanoparticles [20, 36]. Moreover, it is known that the color change was due to the excitation of surface plasmon vibrations with the AgNPs [40, 41].

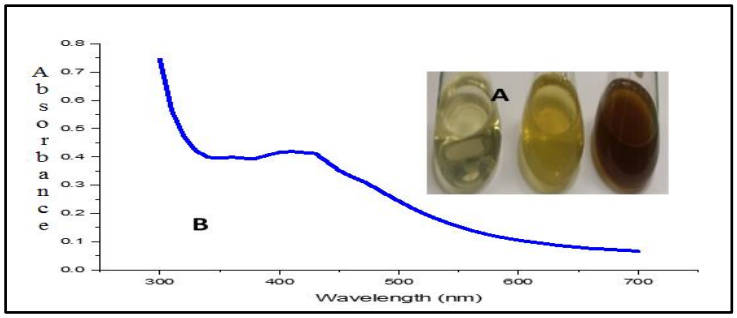

Figure 3. (A) Completion of mixing of the aqueous plant extract and silver nitrate solution was indicated by a color change from yellowish to brown; **(B)** UV-visible spectrum for CgAgNPs showing absorption at wavelength 406 nm.

TEM was used to examine the size and morphology of the synthesized CgAgNPs. The CgAgNPs were spherical with a diameter of 5 to 35 nm (Figure 4A-4D). The morphology of silver nanoparticles in ethanol was observed using TEM (JEOL, Tokyo, Japan). The silver nanoparticles were dispersed in ethanol on a carbon-coated copper TEM grid, and images were acquired. Particle size distribution in ethanol of AgNPs was found to be 10–100 nm (Figure 4B). The XRD pattern was diffraction peaks at (100), (111), (101), (200), (110), (200), (220), and (202), which corresponded to 28°, 32°, 40°, 43°, 48°, 59°, 70°, and 85°, respectively (Figure 4C). AgNPs derived from plant leaf extracts play an important role in improving the biological compatibility of natural products for the treatment of many diseases. The absorbance spectra of AgNPs synthesized with *C. gigantea* will provide clear insights into the surface and size changes of CgAgNPs, and the peak intensity will correlate with the colloidal silver concentration and size disparity. Phytochemical composition of *C. gigantea* leaves is determined by the presence of minerals, amino acids, thiamine, nicotinic acid, and riboflavin [20]. The amino acids present in plant leaf extracts play an important role in the synthesis of AgNPs; this has been confirmed by UV-visible, XRD, and TEM analyses [36].

TEM was used to examine the morphology and size of the biosynthesized CgAgNPs. The results revealed that CgAgNPs were spherical with a diameter ranging from 5 to 35 nm, as shown in Figure 2D. UV–vis spectrum for CgAgNPs showed absorption at a wavelength of 406.00 nm. Changes in permeability may be due to the interaction of nanoparticles with plant compounds [36]. Nanoparticle surfaces adsorb amine, the main agent responsible for reducing silver ions. Furthermore, spherical nanoparticles with minimal agglomeration result from the presence of phytochemical-stabilizing agents in the plant [20].

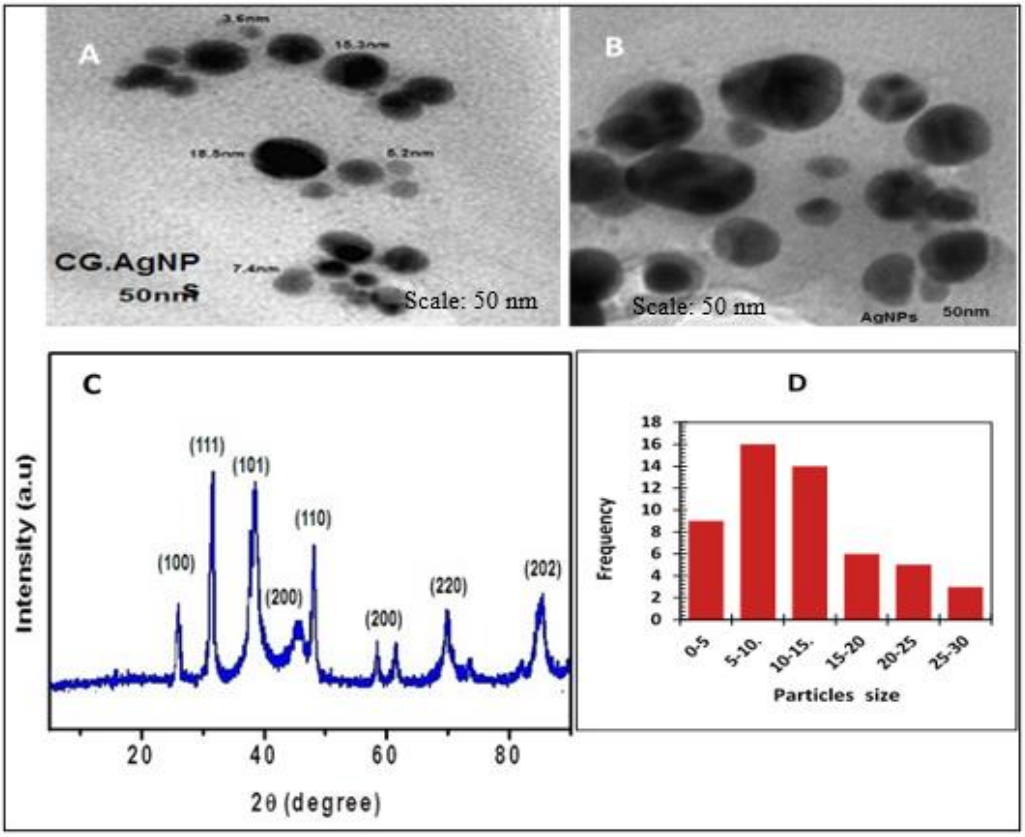

Figure 4. (A) Representative transmission electron microscopy image of CgAgNPs; **(D)** the figure revealed mostly spherical particles in the size range of 5–30 nm; **(B)** AgNPs in a size range of 10–100 nm. Several fields were photographed and used to determine the diameter of the NPs. The images were obtained at an accelerating voltage of 120 kV; **(C)** XRD pattern of synthesized CgAgNPs exhibiting the facets of crystalline silver.

3.5. Effect of ROS on liver cells.

Continuous alterations in ROS function can lead to the development of malignancies. Therefore, to investigate the role of AgNPs and CgAgNPs in inducing oxidative stress in liver cells, ROS levels were measured using carboxy-H_2DCFDA staining and analyzed through spectrofluorometry and fluorescence microscopy. The fluorescent images illustrating ROS generation in liver cells are shown in Figure 5A–D. A quantitative assessment of the significant increase in ROS generation compared with the control groups is summarized in Figure 5E. Following treatment with AgNPs, ROS levels significantly increased in a time- and concentration-dependent manner compared with the CgAgNPs, control, and *C. gigantea* extract groups, which exhibited only minimal fluorescence. In the quantitative fluorescence analysis, the control value was normalized to 100%. A significant ($p < 0.05$) elevation in ROS levels was observed in the AgNPs-positive control group compared with the CgAgNPs and control groups. The maximum increase in ROS generation was 84% with AgNPs (50 mg/kg bw) after 24 h, whereas only an 11% increase was observed with CgAgNPs (100 mg/kg bw) after 24 h. No significant differences were detected between the *C. gigantea* extract group and the control group. The ability of various nanoparticles with different chemical structures to generate ROS, which is closely associated with their cytotoxic effects, has been well-documented in previous studies [33, 34]. The amount of ROS produced by AgNPs is correlated with their shape, size, surface chemistry, and surface area [22], resulting in varying potentials for ROS generation [37].

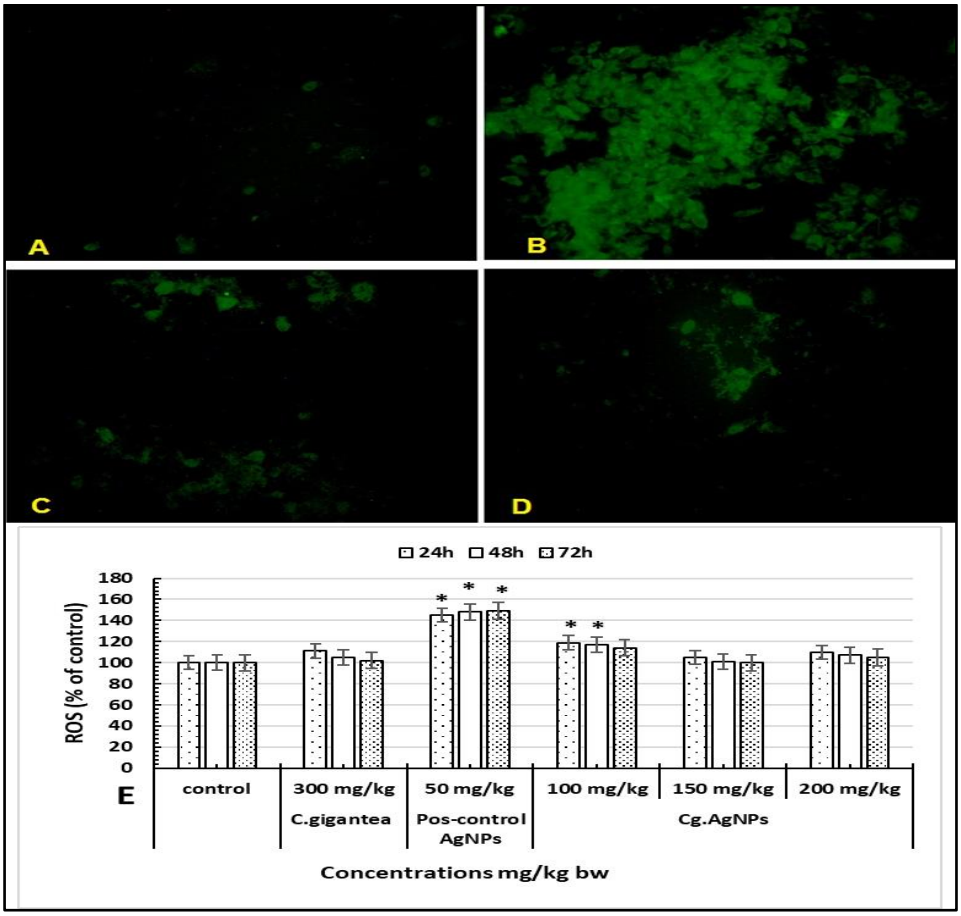

Figure 5. Representative images of liver cells of mice treated for 24 hours, stained with DCF-DA, showing effects of AgNPs, CgAgNPs, and *C. gigantea* on the generation of reactive oxygen species (ROS). **(A)** Control; **(B)** AgNPs (50 mg/kg body weight [bw] of positive control); **(C)** *C. gigantea* (300 mg/kg bw); **(D)** CgAgNPs (200 mg/kg bw). Magnification 40×; **(E)** Increase or decrease of ROS level is shown in percentage relative to the control, which is set at 100%. * Significant ($p < 0.05$).

ROS has multiple functions in cell biology and biochemistry. Therefore, increased ROS generation may be an important factor in inducing processes that contribute to the cytotoxicity and genotoxicity of NP metals, including cellular signal modification, participation in cell death, mutagenesis, proliferation, differentiation, and many disease- and inflammation-related factors [41]. A previous study has expounded the ability of the reactive surfaces of NPs to produce ROS [42]. Despite the presence of surface-dependent chemical compounds and metals, the surface properties of NPs promote rapid ROS generation [39].

The level of ROS processed by CgAgNPs in liver cells of mice was reduced following treatment with *C. gigantea* extract because plants produce a high amount of nonenzymatic antioxidants capable of reducing the oxidative spoilage induced by ROS generation, such as amides, phenolics, flavonoids, lipid peroxides [33], cardiac glycosides, and amino acids [34, 36]. These results were similar to those of previous studies that highlighted the potential role of medicinal plants in curbing ROS generation [42, 43]. The balance between oxidation and reduction is important to maintain a healthy biological system [44]. Oxidative stress results from an imbalance between excessive ROS and/or reactive nitrogen species formation and limited internal defense systems [15]. This imbalance can alter fat, DNA, and proteins, leading to many diseases in humans [39]. In addition, our results showed that the extract of *C. gigantea* leaves possesses antioxidant activity, owing to flavonoids and phenolics that protect cells, similar to previous studies [33].

The observed dose-dependent increases in ROS generation, chromosomal aberrations, and micronuclei in AgNP-treated mice are consistent with well-established mechanisms where oxidative stress initiates mitochondria-mediated apoptosis. For example, Barabadi *et al*. [45] demonstrated that green-synthesized AgNPs induced significant genotoxicity via ROS interaction with DNA and activation of caspase-mediated apoptosis pathways, along with marked antioxidant effects in plant-mediated nanoparticles. Similarly, Al-Asiri *et al*. [46] reported that plant-mediated AgNPs induced cytotoxicity and apoptosis in breast cancer cells through ROS-mediated mitochondrial dysfunction, with upregulation of pro-apoptotic markers (p53, Bax, caspase-3, caspase-9) and downregulation of Bcl-2, supporting the role of ROS-triggered intrinsic apoptosis. In endothelial cells, exposure to AgNPs led to ROS overproduction, resulting in mitochondrial–lysosomal injury, autophagy disruption, and activation of mitochondria-dependent apoptosis; treatment with a ROS scavenger (N-acetylcysteine) attenuated these effects, further implicating ROS as the central trigger.

In contrast, our study shows that administration of *C. gigantea*-derived AgNPs (CgAgNPs) significantly reduces ROS levels, chromosome aberrations, and the incidence of micronuclei in a dose-dependent manner. This suggests that the antioxidant phytochemicals—such as flavonoids and phenolic compounds—in *C. gigantea* can effectively scavenge ROS, stabilize mitochondrial membranes, and inhibit activation of intrinsic apoptotic pathways.

Comparative studies such as Rodríguez-Garraus *et al*. [47] found that the genotoxicity profile of plant-associated AgNP formulations, e.g., combined with kaolin, was milder than chemically synthesized counterparts, with reduced chromosomal damage *in vivo*. These findings parallel our observation that CgAgNPs exhibit a more biocompatible profile than plain AgNPs, highlighting the protective role of plant capping agents. Taken together, suppression of ROS-mediated apoptosis, stabilization of cellular redox balance, and modulation of apoptosis signaling pathways likely mediate the dose-dependent mitigation of oxidative and genotoxic markers by CgAgNPs. Future work should quantify changes in caspase-9 expression,

the Bax/Bcl-2 ratio, and antioxidant enzyme levels (e.g., CAT, GPx) to substantiate these mechanistic insights.

3.6. Chromosome aberration.

A total of 300 chromosomes in metaphase were observed in all groups (n = 6, 50 chromosomes per mouse) to examine structural and numerical aberrations, chromosome type, and chromatid-type aberrations. Chromosome aberrations were observed after AgNPs, CgAgNPs, and C. gigantea extract treatment for 24 h, 48 h, and 72 h, as shown in Table 1 and the representative images in Figure 6A–H. Tests on bone marrow cells showed increased chromosomal aberrations in mice treated with AgNPs, including rings, breaks, fragments, pulverization, centromere adhesion, hypoploidy, polyploidy, and hyperploidy. AgNPs induced a statistically significant number of numerical and structural aberrations in a dose- and time-dependent manner. The frequency of structural aberrations was observed as 23.00 ± 0.4, 22.67 ± 0.5, and 21.67 ± 0.3 in AgNPs (50 mg/kg bw) after 24, 48, and 72 h of exposure, respectively. The control groups showed no significant level ($p < 0.05$) of induced structural chromosome aberration with treatment time. The CgAgNPs-treated groups also showed no significant levels of structural chromosome aberration except at the high dose, with which the maximum aberration frequency was 11.00 ± 0.4 at 200 mg/kg bw after 24 h of treatment. Significant numerical aberrations were also observed in the AgNPs-treated groups, whereas CgAgNPs-treated groups did not show induction of significant aberrations, as seen in Table 1. Moreover, the mitotic index (MI) decreased to 2.5% with increased AgNPs concentration and exposure duration, while it was significantly increased ($p < 0.05$) to 4% in the CgAgNPs-treated groups and approximately 5% in the control groups (Figure 7). *C.gigantea* extract failed to cause chromosomal aberrations compared to the AgNPs groups. The genotoxicity of the extract was evaluated by assessing chromosomal aberrations and conducting a micronucleus assay. The genotoxic potential of AgNPs was reflected in various types of chromosome damage, attributed to oxidation induced by AgNPs.

This study confirmed that AgNPs cause DNA damage, chromosomal aberrations, and other cellular damage, reinforcing conclusions from previous studies [22,48]. *In vivo* and *in vitro* studies have used the chromosomal damage test to detect structural and numerical chromosome aberrations induced by pharmacological and chemical agents [40]. In this study, there was a significant decrease in MI in the AgNPs group compared with the CgAgNPs and control groups; these results are similar to those of Patlolla *et al*. [48]. MI is often used as an important criterion for cell proliferation. It is considered one of the most important indicators of genotoxicity. Hence, the main objective of MI is to guide the prognosis of diseases, including cancer, in patients [49]. Nallanthighal *et al*. [50] reported that orally administered AgNPs may cause oxidative chromosomal aberrations, deletions, and DNA damage in mice, resulting in genome damage, a precursor of carcinogenesis. Our current results showed that *C. gigantea* leaf extract and CgAgNPs failed to cause any chromosomal changes, possibly because of the plant's chemical composition (lipid peroxides, phenolics, and flavonoids), which has antioxidant activity. These results concur with those of previous studies [51, 52].

$$Control: no\ treatment, +ve\ control\ 50 \frac{mg}{kg}\ bw\ AgNPs \quad (1)$$

*Significant ($p < 0.05$) B- Break; R- Ring; F- Fragment; Cd- Centromeric Adhesion; D-Deletion; Pulv- Pulverization; HP-Hypo ploidy; HPr-Hyper ploidy; PP-Poly ploidy; T.h- time (hours).

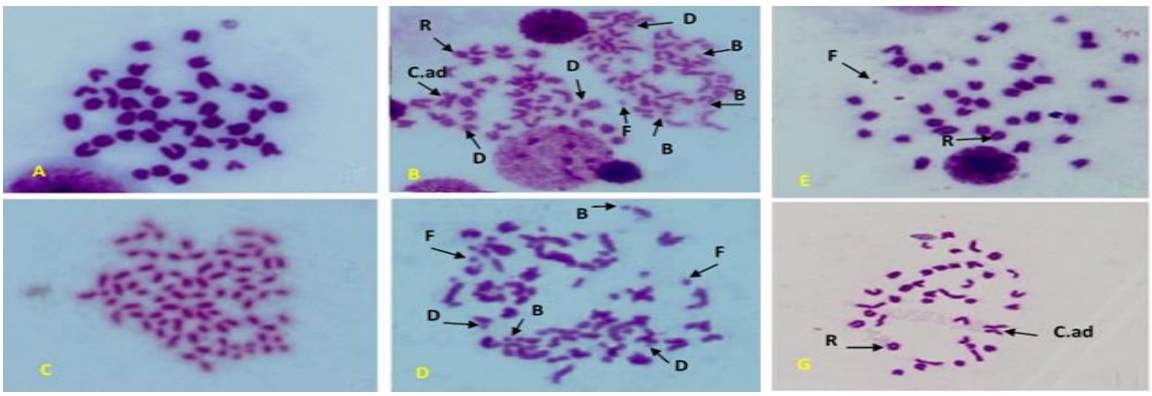

Figure 6. Representative images of bone marrow cells of mice stained with 10% Giemsa stain showing effects of AgNPs, CgAgNPs, and *C. gigantea* on chromosomal aberration. **(A)** Control; **(B)** AgNPs (50 mg/kg body weight [bw]) after 24 h; **(C)** AgNPs (50 mg/kg bw), showing pulverization and polyploidy after 24 h; **(D)** AgNPs (50 mg/kg bw) after 24 h; **(E)** AgNPs (200 mg/kg bw) after 24 h; **(D)** *C.gigantea* (300 mg/kg bw) after 24 h. Magnification 100×. (B, Break; D, Deletion; F, Fragment; C.ad, Centromeric Adhesion; R, Ring). Black arrows indicate chromosomal aberration. Magnification 100×.

Table 1. Chromosome aberrations induced by AgNPs, *C. gigantea*, and CgAgNPs biosynthesis in laboratory mice exposed for 24, 48, and 72 hours.

Groups treatment	T.h	No. Metaphase	Numerical aberrations				Structural aberrations						
			HP	HPr	PP	Mean (%) ± SD	B	R	F	Cd	D	Pulv	Mean (%) ± SD
Control	24	300	4	3	2	3.00±0.2	0	1	2	1	4	1	3.00±0.3
	48	300	5	3	2	3.33±0.3	0	3	2	0	2	2	3.00±0.2
	72	300	4	3	6	4.33±0.2	0	1	1	2	3	2	3.00±0.2
C.gigantea 300mg/kg	24	300	5	2	3	3.33±0.3	0	2	3	1	3	2	3.67±0.3
	48	300	3	1	4	2.67±0.4	0	1	3	2	1	3	3.33±0.2
	72	300	5	2	4	3.67±0.2	0	1	2	2	3	4	4.00±0.3
AgNPs 50mg/kg	24	300	20	21	26	22.33±0.5*	11	11	10	13	9	15	23.00±0.4*
	48	300	21	23	15	19.67±0.2*	5	13	13	11	15	11	22.67±0.5*
	72	300	14	21	13	16.00±0.4*	5	16	9	10	12	13	21.67±0.3*
Cg.AgNPs 100mg/kg	24	300	12	14	9	11.67±0.2*	0	1	2	1	6	6	5.33±0.3
	48	300	14	11	2	9.00±0.3	0	1	1	0	1	6	3.00±0.2
	72	300	6	13	5	8.00±0.5*	0	4	0	4	1	1	3.33±0.4
Cg.AgNPs 150mg/kg	24	300	12	13	12	12.33±0.2*	1	6	3	4	5	6	8.33±0.5
	48	300	9	7	14	10.00±0.6	0	4	3	2	6	6	7.00±0.2
	72	300	8	6	13	9.00±0.2*	0	3	1	5	2	4	5.00±0.2
Cg.AgNPs 200mg/kg	24	300	12	14	16	14.00±0.5*	0	9	3	6	4	11	11.00±0.4*
	48	300	10	11	11	10.67±0.4	0	6	4	5	3	8	8.67±0.3
	72	300	9	11	9	9.67±0.2	0	4	3	5	5	2	6.33±0.2

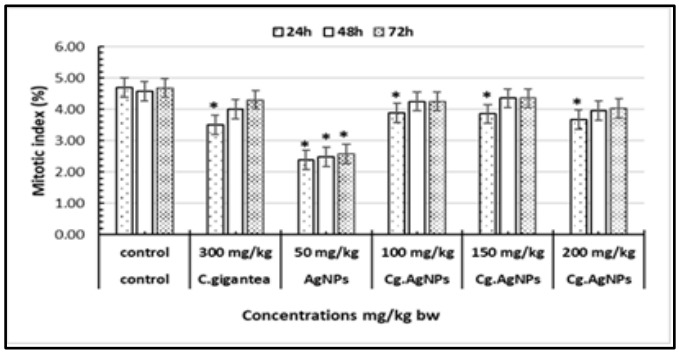

Figure 7. Chromosomal aberrations induced by AgNPs, CgAgNPs, and *C. gigantea* in bone marrow cells of mice after exposure for 24 h, 48 h, and 72 h. Control, normal metaphase chromosomes. * Significant ($p < 0.05$).

3.7. Micronucleus test.

Experimental mice were treated with 50 mg/kg bw of AgNPs for three different durations (24 h, 48 h, and 72 h). A total of 8,000 well-spread metaphases were examined across all groups (n = 4, 2,000 cells per mouse). The number of micronuclei observed after AgNPs

treatment at 24 h, 48 h, and 72 h is presented in Table 2, while representative images of aberrant and normal metaphases are shown in Figure 8. The AgNP-treated groups produced various forms of micronuclei at all time points, with a statistically significant increase ($p < 0.05$). In contrast, the CgAgNP-treated groups exhibited lower micronuclei (MN) levels, although the difference was not statistically significant compared with the control group. The *C. gigantea* extract did not increase MN incidence relative to AgNPs. Micronuclei formation was induced by AgNPs in a time- and dose-dependent manner, accompanied by a reduced PCE/NCE ratio, confirming the genotoxic potential of AgNPs in mice [39, 51]. However, in this study, CgAgNPs neither induced micronuclei formation nor altered the polychromatic erythrocyte/normochromatic erythrocyte (PCE/NCE) ratio. Although limited cytogenetic research has been conducted on *C. gigantea*, our findings confirm that the aqueous extract is non-genotoxic. Moreover, *C. gigantea* aqueous extract exhibited a concentration-dependent anti-mutagenic effect against AgNP-induced chromosomal aberrations, similar to observations in the plant model Allium cepa [51]. These results are consistent with those of Wen *et al*. [22], who reported that AgNP accumulation in immune organs may irritate the spleen and thymus in AgNP-treated groups, but not in those treated with silver ions (Ag). The liver appears to be the most affected organ, showing increased chromosomal damage, polyploidy, and micronuclei formation, indicating nanoparticle-induced genotoxicity. Various mechanisms, such as spindle apparatus disruption and chromosomal breakage, may contribute to MN formation. The *in vivo* micronucleus assay remains a suitable method for evaluating genotoxicity, given the active metabolic, pharmacokinetic, and DNA repair processes [52–54].

In our study, CgAgNPs demonstrated significantly lower genotoxicity compared to chemically synthesized AgNPs, evidenced by reduced micronucleus formation and a stable PCE/NCE ratio. This trend aligns with findings by Gurunathan *et al*. [55], who reported that chemically synthesized AgNPs caused significant DNA fragmentation, ROS generation, and apoptosis in human cells, while biosynthesized AgNPs showed reduced toxicity due to capping with antioxidant phytochemicals [55]. In alignment with our work, Mahmoud *et al*. [56] investigated Salvia officinalis-mediated AgNPs and found reduced oxidative stress, apoptosis, and inflammation in the liver, attributing the biocompatibility to plant-derived antioxidants, which is consistent with our hypothesis regarding *C. gigantea*'s phytochemical contribution [56]. These comparisons reinforce our conclusion that the antioxidant-rich matrix of *C. gigantea* significantly reduces AgNP-induced oxidative and genotoxic effects, making green synthesis a preferable alternative in biomedical applications.

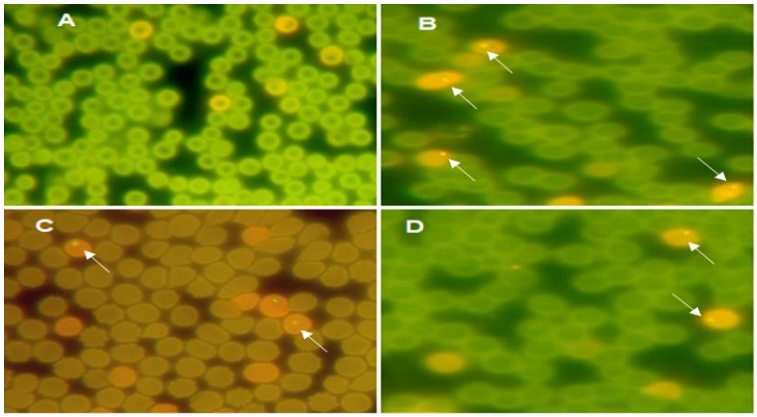

Figure 8. Representative images of peripheral blood cells of mice stained with acridine orange (125 µg/mL in pH 6.8 phosphate buffer), showing effects of AgNPs, *C. gigantea*, and CgAgNPs on the micronucleus (MN). **(A)** Control after 24 h; **(B)** CgAgNPs (50 mg/kg body weight [bw] after 24 h; **(C)** *C. gigantea* (300 mg/kg bw) after 24 h; **(D)** CgAgNPs (200 mg/kg bw) after 24 h. Magnification 40×. White arrows indicate MN.

Table 2. Frequency of micronuclei induced by AgNPs, *C. gigantea*, and CgAgNPs in the peripheral blood of mice exposed to indicated doses for 24, 48, and 72 h duration.

Time	Treatment mg/ kg	N. all cells	N. NCE	N. PCE	N. MN	% MNPCE mean ± SD	% PCE / NCE mean ± SD
24 h	control	8000	7855	145	5	3.45± 0.28	1.85± 0.28*
	300 mg/kg *C. gigantea*	8000	7.860	140	6	4.29± 0.27	1.78± 0.26
	50 mg/kg AgNPs	8000	7923	77	16	20.78± 0.28*	0.97± 0.28*
	100 mg/kg CgAgNPs	8000	7901	99	6	6.06± 0.28	1.25± 0.21*
	150 mg/kg CgAgNPs	8000	7889	111	9	8.11± 0.28*	1.41± 0.22*
	200 mg/kg CgAgNPs	8000	7879	121	11	9.09± 0.28*	1.54± 0.25*
48 h	control	8000	7855	145	5	3.450.38*	1.85±0.28*
	300 mg/kg *C. gigantea*	8000	7862	142	6	4.35± 0.19	1.76± 0.25
	50 mg/kg AgNPs	8000	7914	86	15	17.44.33*	1.09±0.23*
	100 mg/kg CgAgNPs	8000	7909	91	6	6.590.21	1.15±0.21*
	150 mg/kg CgAgNPs	8000	7901	99	9	9.09±0.21	1.25±0.24*
	200 mg/kg CgAgNPs	8000	7891	109	11	10.09±0.25*	1.38±0.32*
72 h	control	8000	7855	145	5	3.45±0.24*	1.85±0.13*
	300 mg/kg *C. gigantea*	8000	7858	142	5	3.52± 0.26	1,81± 0.24
	50mg/kg AgNPs	8000	7910	90	16	17.780.18*	1.14±0.27*
	100 mg/kg CgAgNPs	8000	7888	112	6	5.360.15	1.42±0.29*
	150 mg/kg CgAgNPs	8000	7879	121	9	7.440.39	1.54±0.28*
	200 mg/kg CgAgNPs	8000	7868	132	11	8.330.29	1.68±0.32*

*P < 0.05; 2000 PCE were analyzed for each animal (n=4).

3.8. TUNEL assay (apoptosis).

A dose-dependent increase in TUNEL-positive cells (green fluorescence) was observed in the sections treated with AgNPs, CgAgNPs, and *C. gigantea* for 24 h, as shown in Figures 9A–D. Quantitative estimates of apoptosis relative to the control groups are summarized in Figure 9E. Compared to the control group, the number of apoptotic cells detected by TUNEL staining in the treated groups significantly increased, indicating enhanced apoptotic degeneration of hepatocytes due to CgAgNPs exposure. AgNPs likely induced apoptosis in liver cells by elevating intracellular ROS levels, which can cause DNA damage and trigger cell death [39]. The TUNEL assay detects blunt-ended double-stranded DNA breaks using TdT, which catalyzes the addition of labeled dUTPs to the 3′-hydroxyl termini of DNA fragments. These sites are visualized through reactions with FITC-conjugated antibodies in the liver sections. The TUNEL assay in liver histological sections confirmed apoptosis in the AgNP-treated specimens.

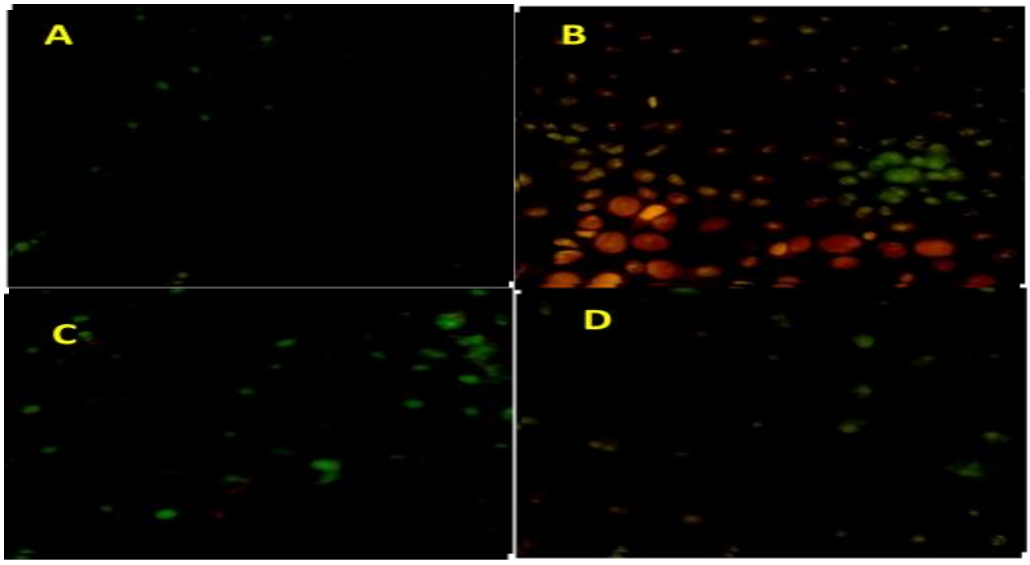

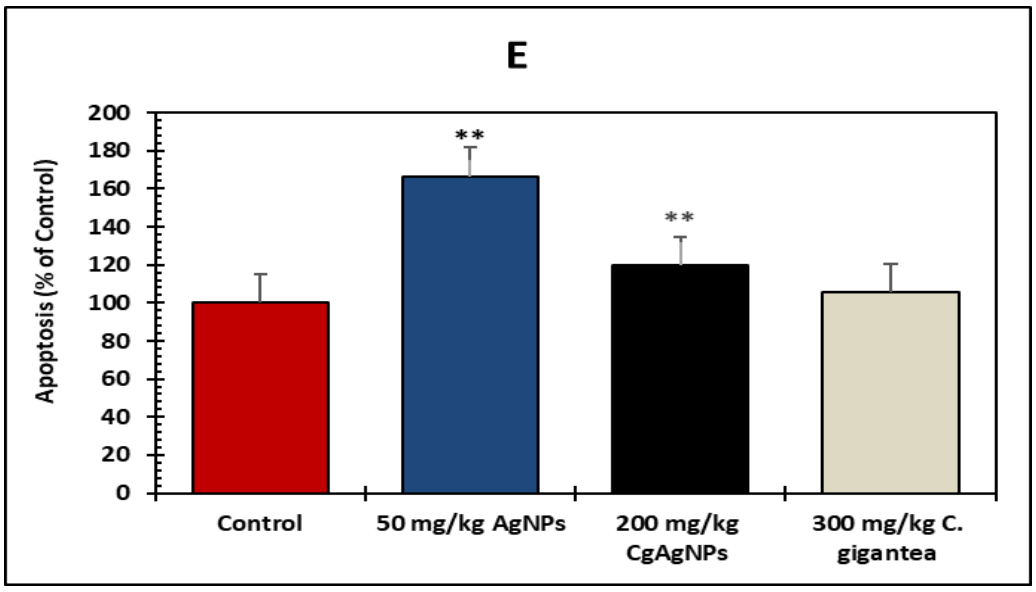

Figure 9. Figures showing the results of TUNEL apoptosis assay (FITC-Labelled) performed on liver sections of control and treated mice for 24h. **(A)** Control: Increase in green fluorescence indicates an increase in TUNEL cells; **(B)** 50 mg/ kg BW AgNPs; decrease in green fluorescence indicates a decrease in TUNEL cells; **(C)** 200 mg/ kg BW CgAgNPs; **(D)** 300 mg/ kg BW *C. gigantea*; **(E)** Increase or decrease in apoptosis level is shown in percentage relative to the control, which is set at 100%. * Significant ($p < 0.05$). Magnification 400X.

In contrast, the CgAgNPs- and *C. gigantea*-treated groups showed very low fluorescence signals under the fluorescence microscope, except at higher doses and longer exposure times, when TUNEL positivity was evident. These findings are consistent with those reported by Al-Anazi *et al*. [39], who observed genotoxic responses induced by AgNPs in mice [53].

4. Conclusions

In conclusion, the results of the current study demonstrated the potential of active biological components in *C. gigantea* as capping and reducing agents to biosynthesize AgNPs. Also, the results of this study demonstrated that CgAgNPs exerted remarkable protective effects against AgNPs-induced toxicity in experimental mice, owing to their antioxidant activity. Therefore, CgAgNPs could be used as a potential natural antioxidant and bioactive compound. In contrast, a marked increase in viable cells was observed with CgAgNPs treatment in all tests. This may lead to the use of natural products to enhance the effectiveness of nanoparticles, as a natural source for treating incurable diseases such as cancer, because it contains dozens of phenolic compounds, enzymes, and plant hormones. These interact with both the silver ions we use and the cell signaling pathways we aim to control with AgNPs in the cell. Future research should focus on evaluating the long-term effects of exposure and tissue-specific responses to CgAgNPs better to understand their safety and efficacy in clinical settings.

Author Contributions

Conceptualization, M.A.H.A. and A.A.A.; methodology, A.A.A. and H.M.A.A.; software, M.A.H.A.; validation, M.A.H.A. and A.A.A.; formal analysis, M.A.H.A. and A.A.A.; investigation, M.A.H.A. and A.A.A.; resources, M.A.H.A. and A.A.A.; data curation, Y.M.S.J. and H.M.A.A.; writing—original draft preparation, Y.M.S.J. and A.A.A.; writing—review and

editing, M.A.H.A.; visualization, M.A.H.A.; project administration, M.A.H.A. All authors have read and agreed to the published version of the manuscript."

Institutional Review Board Statement

The animal study protocol was approved by the Ethics Committee of Thamar University Ethics Reference No. SE-19-127.

Informed Consent Statement

Not applicable.

Data Availability Statement

Data supporting the findings of this study are available upon reasonable request from the corresponding author.

Funding

Funding is not available for this search.

Acknowledgments

Not applicable

Conflicts of Interest

The authors declare that they have no known competing financial interests or personal relationships that could have influenced the work reported in this paper.

References

1. Al-Maydama, H. M.A.; Jamil, Y. M.S.; Awad, M.A.H.; Abduljabbar, A. A. M. Electrochemical investigations and antimicrobial activity of Au nanoparticles photodeposited on titania nanoparticles. *Heliyon* **2024**, *10*, e23722, https://doi.org/10.1016/j.heliyon.2023.e23722.
2. Jamil, Y. M. S.; Awad, M. A. H.; Al-Maydama, H. M. A.; EL-Ghoul, Y.; Al-Hakimi, A. N. Synthesis and study of enhanced electrochemical properties of NiO nanoparticles deposited on TiO_2 nanotubes. *Appl. Organomet. Chem.* **2022**, *36*, e6795, https://doi.org/10.1002/aoc.6795.
3. Jamil, Y.M.S.; Awad, M.A.H.; Al-Maydama, H.M.A. Physicochemical Properties and Antibacterial Activity of Pt Nanoparticles on TiO_2 Nanotubes as Electrocatalyst for Methanol Oxidation Reaction. *Results Chem.* **2022**,*4*, 100531, https://doi.org/10.1016/j.rechem.2022.100531.
4. Jamil, Y.M.S.; Awad, M.A.H.; Al-Maydama, H.M.A.; Alhakimi, A.N.; Shakdofa, M.M.E.; Mohammed, S.O. Gold nanoparticles loaded on TiO_2 nanoparticles doped with N_2 as an efficient electrocatalyst for glucose oxidation: preparation, characterization, and electrocatalytic properties. *J. Anal. Sci. Technol*. **2022**, *13*, 54, https://doi.org/10.1186/s40543-022-00363-0.
5. Jamil. Y.M.S.; Awad. M.A.H.; Al-Maydama. H.M.A. Electrochemical and Catalytic Properties of Au Nanoparticles. *Sana'a Univ. J. Appl. Sci. Technol.* **2023**, *1*, 53 – 69, http://dx.doi.org/10.59628/jast.v1i1.153.
6. Azwanida, N.N. A review on the extraction methods use in medicinal plants, principle, strength and limitation. *Med. Aromat. Plants.* **2015**, *4*, 2167-0412, http://dx.doi.org/10.4172/2167-0412.1000196.
7. Ali, A.Q.; Farah, M.A.; Abou-Tarboush, F.M.; Al-Anazi, K.M.; Ali, M.A.; Lee, J.; Hailan, W.A.Q.; Mahmoud, A.H. Cytogenotoxic effects of *Adenium obesum* seeds extracts on breast cancer cells. *Saudi J. Biol. Sci.* **2019**, *26*, 547–553, https://doi.org/10.1016/j.sjbs.2018.12.014.

8. Sharma, V.; Kaushik, S.; Pandit, P.; Dhull, D.; Yadav, J.P.; Kaushik, S. Green synthesis of silver nanoparticles from medicinal plants and evaluation of their antiviral potential against chikungunya virus. *Appl. Microbiol. Biotechnol*. **2019**, *103*, 881–891, https://doi.org/10.1007/s00253-018-9488-1.
9. Raja, R.R.; Kishore, N.; Sreenivasulu, M.; RasoolBee, S.K.; Nandini, S.; Ooha, L.; Chaitanya, N. *Calotropis gigantea*- botanical, pharmacological view. *J. Med. Plant Stud.* **2016**, *4*, 87–89.
10. Upadhyay, R.K. Ethnomedicinal, pharmaceutical and pesticidal uses of *Calotropis procera* (Aiton) (Family: Asclepiadaceae*). Int. J. Green Pharm*. **2014**, *8*, 135-146.
11. Singh, S.; Pathaka, S.; Agrawalb, N.; Maitic, P.P. Correlation between *in vitro* antioxidant activity and GC-MS evaluation of *Calotropis gigantea* (L.) R. Br. root extract. *J. Indian Chem. Soc* **2020**, *97*, 2311-2320.
12. Rathod, N.R.; Chitme, H.R.; Irchhaiya, R.; Chandra, R. Hypoglycemic effect of *Calotropis gigantea* Linn. leaves and flowers in streptozotocin-induced diabetic rats. *Oman Med. J*. **2011**, *26*, 104–108, https://doi.org/10.5001/omj.2011.26.
13. Mishra, P.K.; Thawani, V. Characterization of *Alternaria alternata* isolated from *Calotropis gigantea* plant leaf. *Int. J. Curr. Microbiol. Appl. Sci.* **2016**, *5*, 459–466, http://dx.doi.org/10.20546/ijcmas.2016.510.052.
14. Jacinto, S.D.; Chun, E.A.C.; Montuno, A.S.; Shen, C.C.; Espineli, D.L.; Ragasa, C.Y. Cytotoxic cardenolide and sterols from *Calotropis gigantea*. *Nat. Prod. Commun*. **2011**, *6*, 803–806, https://doi.org/10.1177/1934578X1100600614.
15. Al-Mareed, A.A.; Farah, M.A.; Al-Anazi, K.M.; Hailan, W.A.Q.; Ali, M.A. Potassium bromate-induced oxidative stress, genotoxicity and cytotoxicity in the blood and liver cells of mice. *Mutat. Res. - Genet. Toxicol. Environ. Mutagen*. **2022**, *878*, 503481, https://doi.org/10.1016/j.mrgentox.2022.503481.
16. Kemala, P.; Idroes, R.; Khairan, K.; Ramli, M.; Jalil, Z.; Idroes, G. M.; Tallei, T. E.; Helwani, Z.; Safitri, E.; Iqhrammullah, M.; & Nasution, R. Green Synthesis and Antimicrobial Activities of Silver Nanoparticles Using Calotropis gigantea from Ie Seu-Um Geothermal Area, Aceh Province, Indonesia. Molecules, **2022**, 27(16), 5310. https://doi.org/10.3390/molecules27165310.
17. Rengarajan, S.; Sivalingam, A. M.; Pandian, A.; & Chaurasia, P. K. Nanomaterial (AgNPs) Synthesis Using Calotropis gigantea Extract, Characterization and Biological Application in Antioxidant and Antibacterial Activity. Journal of Inorganic and Organometallic Polymers and Materials, **2024**, 34(9), 4005–4021. https://doi.org/10.1007/s10904-024-03058-8.
18. Abdallah, B. M.; & Ali, E. M. Therapeutic Effect of Green Synthesized Silver Nanoparticles Using Erodium glaucophyllum Extract against Oral Candidiasis: In Vitro and *In vivo* Study. Molecules, **2022**, 27(13), 4221. https://doi.org/10.3390/molecules27134221.
19. Zhao, Z.; Yan, J.; Wang, T.; Ma, Y.; Xie, M.; Mu, X.; Wang, X.; Zheng, Z.; Li, Y.; Li, G. Multi-functional Calotropis gigantea fabric using self-assembly silk fibroin, chitosan, and nano-silver microspheres with oxygen low-temperature plasma treatment. *Colloids Surf. B: Biointerfaces*. **2022**, *215*, 112488, https://doi.org/10.1016/j.colsurfb.2022.112488.
20. Aina, D.A.; Animashaun, O.H. Calotropis procera mediated synthesis of silver nanoparticles and its antibacterial effect on selected pathogens. *Asian Plant Res. J.* **2024**, *12*, 69–77, https://doi.org/10.9734/aprj/2024/v12i6282.
21. Ali, E. M.; & Abdallah, B. M. Effective inhibition of candidiasis using an eco-friendly leaf extract of calotropis-gigantean-mediated silver nanoparticles. Nanomaterials, **2020**, 10 (3), 422. https://doi.org/10.3390/nano10030422.
22. Wen, H.; Dan, M.; Yang, Y.; Lyu, J.; Shao, A.; Cheng, X.; Chen, L.; Xu, L. Acute toxicity and genotoxicity of silver nanoparticle in rats. *PloS One* **2017**, *12*, 1–16, https://doi.org/10.1371/journal.pone.0185554.
23. Siddiqi, K.S.; Husen, A.; Rao, R.A.K. A review on biosynthesis of silver nanoparticles and their biocidal properties. *J. Nanobiotechnol*. **2018**, *16*, 11-14, https://doi.org/10.1186/s12951-018-0334-5.
24. Dobrzynska, M.M.; Gajowik, A.; Radzikowska, J.; Lankoff, A.; Dusinska, M.; Kruszewski, M. Genotoxicity of silver and titanium dioxide nanoparticles in bone marrow cells of rats *in vivo*. *Toxicology* **2014**, *315*, 86–91, https://doi.org/10.1016/j.tox.2013.11.012.
25. Piao, M.J.; Kang, K.A.; Lee, I.K.; Kim, H.S.; Kim, S.; Choi, J.Y.; Choi, J.; Hyun, J.W. Silver nanoparticles induce oxidative cell damage in human liver cells through inhibition of reduced glutathione and induction of mitochondria-involved apoptosis. *Toxicol. Lett*. **2011**, *201*, 92–100, https://doi.org/10.1016/j.toxlet.2010.12.010.
26. Li, J.K.; Liu, X.D.; Shen, L.; Zeng, W.M.; Qiu, G.-Z. Natural plant polyphenols for alleviating oxidative damage in man: Current status and future perspectives. *Trop. J. Pharm. Res*. **2016**, *15*, 1089–1098, http://dx.doi.org/10.4314/tjpr.v15i5.27.

27. Liu, Y.X.; Karsai, A.; Anderson, D.S.; Silva, R.M.; Uyeminami, D.L.; Van Winkle, L.S.; Pinkerton, K.E.; Liu, G.Y. Single-cell mechanics provides an effective means to probe *in vivo* interactions between alveolar macrophages and silver nanoparticles. *J. Phys. Chem. B.* **2015**, *119*, 15118–15129. https://doi.org/10.1021/acs.jpcb.5b07656.
28. Poirier, M.; Simard, J.C.; Girard, D. Silver nanoparticles of 70 nm and 20 nm affect differently the biology of human neutrophils. *J. Immunotoxicol*. **2016**, *13*, 375–385, https://doi.org/10.3109/1547691X.2015.1106622.
29. Han, J.W.; Jeong, J.K.; Gurunathan, S.; Choi, Y.J.; Das, J.; Kwon, D.N.; Cho, S.G.; Park, C.; Seo, H.G.; Park, J.K.; Kim, J.H. Male-and female-derived somatic and germ cell-specific toxicity of silver nanoparticles in mouse. *Nanotoxicology* **2016**, *10*, 361–373, https://doi.org/10.3109/17435390.2015.1073396.
30. Raj, A.; Shah, P.; Agrawal, N. Dose-dependent effect of silver nanoparticles (AgNPs) on fertility and survival of Drosophila: An in-vivo study. *PloS One* **2017**, *12*, e0178051, https://doi.org/10.1371/journal.pone.0178051.
31. Younas, W.; Khan, F. U.; Zaman, M.; Lin, D.; Zuberi, A.; & Wang, Y. Toxicity of synthesized silver nanoparticles in a widespread fish: A comparison between green and chemical. Science of The Total Environment, **2022**, 845, 157366, https://doi.org/10.1016/j.scitotenv.2022.157366.
32. Ribeiro, L. G.; Barbieri, E.; & de Souza, A. O. Assessment of the toxicity of bio-synthesized silver nanoparticles on Oreochromis niloticus (Nile tilapia). Environmental Science: Nano, **2025**, 12(6), 3173–3181, https://doi.org/10.1039/d4en01125b.
33. Mahato, K.; Kakoti, B.B.; Borah, S.; Kumar, M. In-vitro antioxidative potential of methanolic aerial extracts from three ethnomedicinal plants of Assam: A Comparative Study. *J. Appl. Pharm. Sci.* **2015**, *12*, 111-116, https://doi.org/10.7324/JAPS.2015.501219.
34. Kumar, N.S.; Balamurugan, V. In-vitro antioxidant activity, total phenolic and total flavonoid contents of flower extract of *Calotropis gigantea*. *Res. J. Phytochem*. **2015**, *9*, 137-143, https://doi.org/10.3923/rjphyto.2015.137.143.
35. Al-Qudah, M.A.; Allahham, F.E.; Obeidat, S.M.; Al-Jaber, H.I.; Lahham, J.N.; Abu Orabi, S.T. In vitro antioxidant activities, total phenolics and total flavonoids of the different extracts of Capparis spinosa L. and Capparis decidua Edgew (forssk.) from Jordan. *Int. J. Pharm. Res.* **2020**, *12*, 1226–1236, http://doi.org/10.31838/ijpr/2020.12.03.183.
36. Farah, M.A.; Ali, M.A.; Chen, S.M.; Li, Y.; Al-Hemaid, F.M.; Abou-Tarboush, F.M.; Al-Anazi, K.M.; Lee, J. Silver nanoparticles synthesized from *Adenium obesum* leaf extract induced DNA damage, apoptosis and autophagy via generation of reactive oxygen species. *Colloids Surf. B. Biointeraces.* **2016**, *141*, 158–169, https://doi.org/10.1016/j.colsurfb.2016.01.027.
37. Stankov-Jovanović, V.P.; Ilić, M.D.; Mitić, V.D.; Mihajilov-Krstev, T.M.; Simonović, S.R.; Nikolić Mandić, S.D.; Cole, R.B. Secondary metabolites of Seseli rigidum: Chemical composition plus antioxidant, antimicrobial and cholinesterase inhibition activity. *J. Pharm. Biomed. Anal.* **2015**, *111*, 78-90, https://doi.org/10.1016/j.jpba.2015.03.015.
38. Al-Dalahmeh, Y.; Al-Bataineh, N.; Al-Balawi, S.S.; Lahham, J.N.; Al-Momani, I.F.; Al-Sheraideh, M.S.; Mayyas, A.S.; Abu Orabi, S.T.; Al-Qudah, M.A. LC-MS/MS Screening, Total Phenolic, Flavonoid and Antioxidant Contents of Crude Extracts from Three Asclepiadaceae Species Growing in Jordan. *Molecules* **2022**, *27*, 859, https://doi.org/10.3390/molecules27030859.
39. Binz, R.L.; Pathak, R. Protocol for preparation and staining of chromosomes isolated from mouse and human tissues for conventional and molecular cytogenetic analysis. *STAR Protocols* **2024**, *5*, 102897, https://doi.org/10.1016/j.xpro.2024.102897.
40. Pinto, S.R.; Helal-Neto, E.; Paumgartten, F.; Felzenswalb, I.; Araujo-Lima, C.F.; Martínez-Máñez, R.; Santos-Oliveira, R. Cytotoxicity, genotoxicity, transplacental transfer and tissue disposition in pregnant rats mediated by nanoparticles: the case of magnetic core mesoporous silica nanoparticles. *Artif. Cells Nanomed. Biotechnol.* **2018**, *46*, 527–538, https://doi.org/10.1080/21691401.2018.1460603.
41. Zhang, C.; Wang, X.; Du, J.; Gu, Z.; Zhao, Y. Reactive oxygen species-regulating strategies based on nanomaterials for disease treatment. *Adv. Sci.* **2021**, *8*, 2002797, https://doi.org/10.1002/advs.202002797.
42. Abdal Dayem, A.; Hossain, M.; Lee, S.; Kim, K.; Saha, S.; Yang, G.M.; Choi, H.Y; Cho, S.G. The role of reactive oxygen species (ROS) in the biological activities of metallic nanoparticles. *Int. J. Mol. Sci.* **2017**, *18*, 109–120, https://doi.org/10.3390/ijms18010120.

43. Tufarelli, V.; Casalino, E.; D'Alessandro, A.G.; Laudadio, V. Dietary phenolic compounds: biochemistry, metabolism and significance in animal and human health. *Curr. Drug Metab*. **2017**, *18*, 905–913, https://doi.org/10.2174/1389200218666170925124004.
44. Kasote, D.M.; Katyare, S.S.; Hegde, M.V.; Bae, H. Significance of antioxidant potential of plants and its relevance to therapeutic applications. *Int. J. Biol. Sci.* **2015**, *11*, 982, https://doi.org/10.7150/ijbs.12096.
45. Barabadi, H.; Nasab, M.N.; Sanami, S.; Mahjoub, M.A.; Azarnezhad, A.; Jabbari, N.; Ovais, M.; Saravanan, M. Bioinspired green-synthesized silver nanoparticles: Genotoxicity, antidiabetic, antioxidant, and antimicrobial assessment. *Mater. Adv.* **2023**, *4*, 1753–1768, https://doi.org/10.1039/D3MA00089C.
46. Al-Asiri, W.Y.; Ahmed, M.S.; Al-Harbi, A.A.; Iqbal, D.; Alqahtani, S.A.; Mohamed, S.A. Cytotoxic and apoptotic effects of green synthesized silver nanoparticles via reactive oxygen species–mediated mitochondrial pathway in human breast cancer cells. *Cell Biochem. Funct.* **2024**, *42*, e413, https://doi.org/10.1002/cbf.4113.
47. Rodríguez-Garraus, A.; de Miguel, T.; Alonso, M. L.; Catalán, J.; López de Cerain, A.; Azqueta, A. Genotoxicity and toxicity assessment of a formulation containing silver nanoparticles and kaolin: An *in vivo* integrative approach. *Nanomaterials* **2023**, *13*, 3, https://doi.org/10.3390/nano13010003.
48. Patlolla, A.K.; Hackett, D.; Tchounwou, P.B. Genotoxicity study of silver nanoparticles in bone marrow cells of Sprague–Dawley rats. *Food Chem. Toxicol.* **2015**, *85*, 52–60, https://doi.org/10.1016/j.fct.2015.05.005.
49. Hailan, W.A.; Al-Anazi, K.M.; Farah, M.A.; Ali, M.A.; Al-Kawmani, A.A.; Abou-Tarboush, F.M. Reactive Oxygen Species-Mediated Cytotoxicity in Liver Carcinoma Cells Induced by Silver Nanoparticles Biosynthesized Using Schinus molle Extract. *Nanomaterials* **2022**, *12*, 161, https://doi.org/10.3390/nano12010161.
50. Nallanthighal, S.; Chan, C.; Murray, T.M.; Mosier, A.P.; Cady, N.C.; Reliene, R. Differential effects of silver nanoparticles on DNA damage and DNA repair gene expression in Ogg1-deficient and wild type mice. *Nanotoxicology*. **2017**, *11*, 996–1011, https://doi.org/10.1080/17435390.2017.1388863.
51. Mansour, H.A.; Mahfouz, H.; Maher, N. Anti-mutagenic potential of algal extracts on chromosomal aberrations in *Allium cepa*. *Acta. Biol. Hung.* **2017**, *68*, 137–149, https://doi.org/10.1556/018.68.2017.2.2.
52. Hayashi, M. The micronucleus test—most widely used *in vivo* genotoxicity test. *Gene. Environ.* **2016**, *38*, 1–18, https://doi.org/10.1186/s41021-016-0044-x.
53. Kim, Y.J.; Rahman, M.M.; Lee, S.M.; Kim, J.M.; Park, K.; Kang, J.H.; Seo, Y.R. Assessment of *in vivo* genotoxicity of citrated-coated silver nanoparticles via transcriptomic analysis of rabbit liver tissue. *Int. J. Nanomedicine*. **2019**, *14*, 393–405, https://doi.org/10.2147/IJN.S174515.
54. Al-kawmani, A.A.; Alanazi, K.M.; Farah, M.A.; Ali, M.A.; Hailan, W.A.Q.; Al-Hemaid, F.M. Apoptosis-Inducing Potential of Biosynthesized Silver Nanoparticles in Breast Cancer Cells. *J. King Saud Univ.-Sci.* **2020**, *32*, 2480–2488, http://doi.org/10.1016/j.jksus.2020.04.002.
55. Gurunathan, S, Park, J.H.; Han, J.W.; Kim, J.H. Comparative assessment of the apoptotic potential of silver nanoparticles synthesized by Bacillus tequilensis and chemically synthesized nanoparticles in MDA-MB-231 breast cancer cells. Int. J. Nanomed. **2015**, *10*, 4203-4223, https://doi.org/10.2147/IJN.S83953.
56. Metwally, D. M.; Alajmi, R. A.; El-Khadragy, M. F.; & Al-Quraishy, S. Silver Nanoparticles Biosynthesized With Salvia officinalis Leaf Exert Protective Effect on Hepatic Tissue Injury Induced by Plasmodium chabaudi. Frontiers in Veterinary Science, **2021**, 7, https://doi.org/10.3389/fvets.2020.620665.

Publisher's Note & Disclaimer